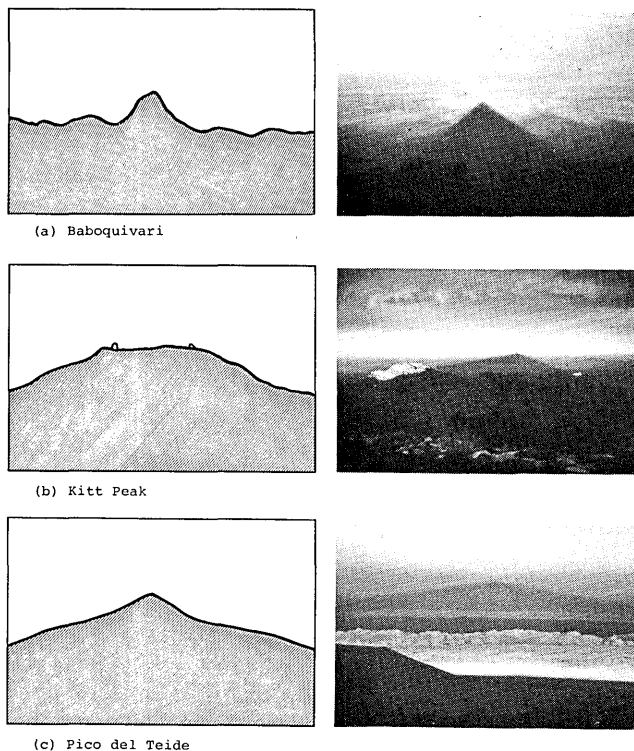


Mountain shadow phenomena

William Livingston and David Lynch



Regardless of profile, whether flat topped or pointed, to the summit observer all mountain peaks cast triangular shadows when the sun is low. A theory for such anomalous shadows is developed. The shadow apex angle is shown to depend only on the ratio of the breadth of the mountain to its height.

Problem

From a lifetime of experience we know that our shadow out-of-doors mimics our own form. Similarly the shadows of nearby objects such as buildings follow their outline. If a shadow is cast some distance it becomes less distinct, of course, because the sun is not a point source but rather subtends an angle of about 0.5° . These are the expected conditions. Thus we find ourselves puzzled when, from the summit of a flat-topped mountain at sunset, the mountain's shadow is seen to be pyramidal in shape and remarkably sharp in outline.

Figure 1 contains photographs of the shadows of several peaks whose profiles are sketched to the left. Their shadows are very similar in form despite the extreme disparity in originating silhouette. From these

Fig. 1. Photographs of the shadow of (a) Baboquivari by K. DeGioia, (b) Kitt Peak, and (c) Pico del Teide by M. Cohen. To the left are the respective profiles that give rise to their shadows.

and other observations we conclude that when viewed from (or near) the summit at a time of low sun (1) almost all mountains cast triangular shadows bearing no relation to the immediate terrain; (2) each mountain has a characteristic apex angle to the shadow which is independent of the sun's altitude or even the exact position of the observer (the shadow apex angle of the huge volcano Mauna Loa being constant within 10 miles of the summit); and (3) the shadow in the vicinity of the antisolar point appears strangely narrow ($<0.5^\circ$).

The literature contains many photographs of mountain shadows, but their anomalous character does not seem to have been previously recognized.¹⁻³ The shadow of Mt. Fuji (Fig. 2) is sufficiently famous to even have its own name, the Kage-Fuji.⁴ But even the near pyramidal Fuji does not replicate in its shadow. (The summit caldera, 800 m in breadth is missing, and the shadow sides are straight not gracefully curved as are its slopes.) Presumably analogous questions will arise when we attempt to interpret shadow pictures from future planetary landers. How can we reconcile these observations with the laws of geometric optics?

William Livingston is with Kitt Peak National Observatory, P.O. Box 26732, Tucson, Arizona 85726; David Lynch is with California Institute of Technology, Physics Department, Pasadena, California 91125.

Received 25 May 1978.

0003-6935/79/030265-05\$00.50/0.

© 1979 Optical Society of America.

Explanation

Qualitatively the absence of summit detail in a shadow is a matter of perspective. At low sun the origin of any features seen near the antisolar point is many kilometers distant. The sides of a mountain line up toward this vanishing point, and all summit structure is compressed into that convergence point, losing identity because of distance and the 0.5° nonparallelism of the rays.

We find an explanation of the pyramidal shape requires an analytic approach. Consider an observer situated atop a mountain Z_t , which we shall choose to be 2-D in the x - z plane and located on the origin of a 3-D Cartesian coordinate system (Fig. 3). The sun S is at an elevation α in the y - z plane and casts the shadow of the mountain on the horizontal x - y plane. For simplicity let us investigate a symmetric mountain whose profile is $H(x)$ and whose width as a function of height is $W(z)$. $W(z)$ can be obtained from the inversion of $H(x)$. The shape of the mountain shadow $H'(x)$ is a linear projection of $H(x)$ on the x - y plane. The two profiles are related point-by-point via

$$\tan\alpha = H(x)/H'(x). \quad (1)$$

The width of the shadow is $W'(y)$. $W(z)$ and $W'(y)$ have the same functional form, but their independent variables are scaled by $\tan\alpha$:

$$z = y \tan\alpha. \quad (2)$$

From the top of the mountain Z_t , $H'(x)$ is stretched and appears greatly foreshortened. Let us define a dimensionless width variable $\omega(y)$, which we conveniently choose to be equal to the angular width of the shadow as seen from $Z(t)$, i.e.,



Fig. 2. The remarkable Kage-Fuji, or shadow of Mt. Fuji (*Japan Times* photograph).

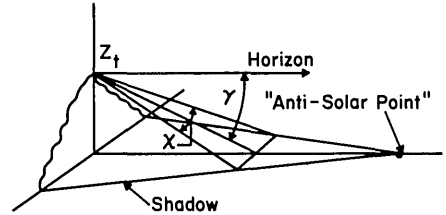
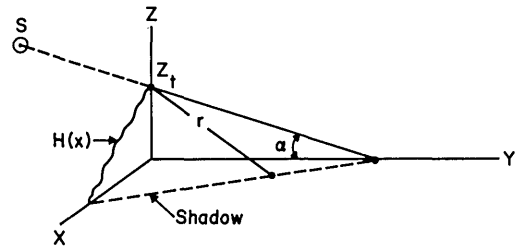


Fig. 3. Coordinate systems: For derivations (upper) and for the observer (lower).

$$\omega(y) = \sin^{-1} \left[\frac{W'(y)}{r} \right] = \sin^{-1} \left[\frac{W'(y)}{(x^2 + y^2 + Z_t^2)^{1/2}} \right], \quad (3)$$

where ω is measured in units of χ , the horizontal angular coordinate. For low sun angles $x \ll y$ except very near the base of the mountain. Thus we may drop x from Eq. (3). Also, since we are most interested in the shape of the shadow in the vicinity of the horizon, $\omega(y)$ will be small, and thus Eq. (3) becomes

$$\omega(y) \approx [W'(y)]/(y^2 + Z_t^2)^{1/2}. \quad (4)$$

The coordinate y is not useful for this problem because it appears distorted. Let us transform to another angular coordinate γ ,

$$\gamma = Z_t/y, \quad (5)$$

where γ is the angular distance below the horizon. We now have the problem defined in dimensionless observer coordinates χ and γ . The angular width then becomes

$$\omega(\gamma) \approx \frac{W'(\gamma)}{r} \approx \frac{W'(\gamma)}{(Z_t^2 + Z_t^2/\gamma^2)^{1/2}}. \quad (6)$$

Let us define a convergence function $C_{Z_t}(\gamma)$:

$$C_{Z_t}(\gamma) = \frac{1}{Z_t} \frac{1}{(1 + 1/\gamma^2)^{1/2}}, \quad (7)$$

with Z_t as a parameter. For small values of γ ($\gamma < 0.5$ rad), $C_{Z_t}(\gamma) \approx \gamma/(Z_t)$. The observed shape of the mountain shadow is given by

$$\omega(\gamma) = W'(\gamma)C_{Z_t}(\gamma). \quad (8)$$

Since $C_{Z_t}(\gamma) \approx \gamma/(Z_t)$, the width of the shadow is scaled by γ , which is essentially a triangular function. This explains the characteristic shape of mountain shadows. $C_{Z_t}(\gamma)$ dominates $W'(\gamma)$, and the actual shape of the mountain plays only a minor role. Foreshortening and distortion occur according to Eq. (5). Except for the small influence of $W(\gamma)$ and $\omega(\gamma)$, the convergence of

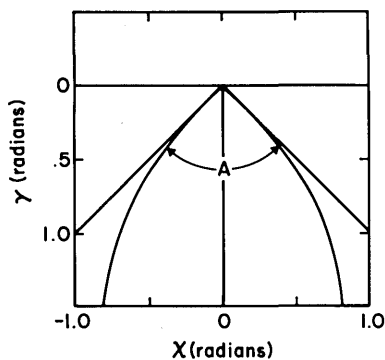


Fig. 4. Shadow width (χ) as a function of dip below the horizon (γ) in the observer's coordinates.

Table I. Comparison of the Calculated and Observed Shadow Apex Angle A

	Width		Elevations		Shadow apex angle	
	W	Base	Summit	Calc.	Obs.	
Mt. Fuji, Japan	(km)	(m)	(m)	(deg)	(deg)	
Baboquivari, Ariz.	6.1	800	3778	125	128	
Kitt Peak, Ariz.	0.64	1830	2356	105	101	
Pico del Teide, Canary Islands	3.1	1070	2095	149	143	
Mauna Loa, Hawaii	6.3	2200	3718	168	163	
White Mountain, Calif.	13.7	2743	4064	169	169	
	∞	3861	3861	180	180	

Data on the mountain width and elevations are taken from topographical maps. Width is the north-south dimension at the immediate base. The width of White Mountain is so labeled because it is an extended ridge.

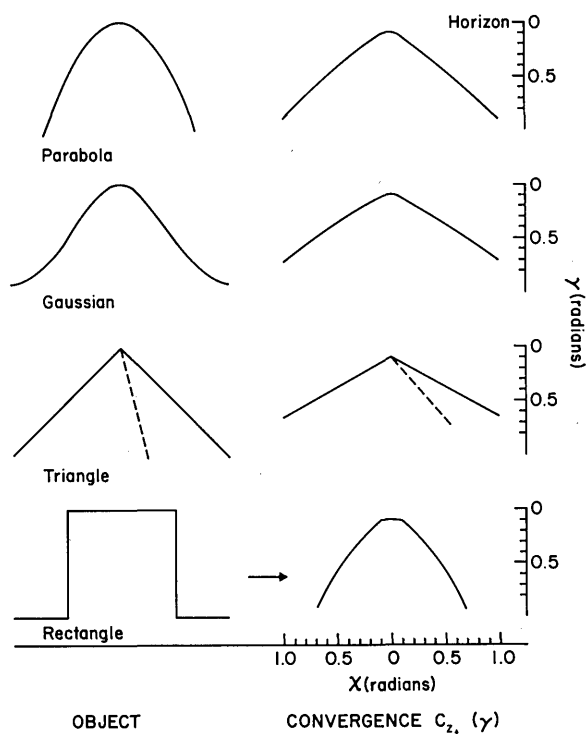


Fig. 5. Examples of how the convergence function transforms various input geometries.

mountain shadows is closely analogous to the apparent convergence of long straight railroad tracks (Fig. 4).

The apex angle A depends on the height of the observer relative to the width of the mountain, and to a lesser degree on the true profile of the mountain. Since all mountains are wider at the bottom than at the top they tend to have pointy shadows. Defining \bar{W} as the width of the mountain at $z = Z_t/2$, A is approximately

$$A \approx 2 \tan^{-1}(\bar{W}/Z_t). \quad (9)$$

Note that A is not a function of α . Table I compares the calculated and observed values of A , and we see the agreement is close, which supports this theory.

To demonstrate the effect of perspective on the apparent shapes of mountain shadows, $\omega(\gamma)$ has been calculated for several profiles $H(x)$, including a parabola, a Gaussian, a symmetric and asymmetric triangle, and a rectangle. For comparison all profiles have $Z_t/W = 0.5$, and $\alpha = 5^\circ$. Figure 5 shows these profiles and the corresponding shadows as seen by an observer located at the summit.

Sharpness of the Shadow

It is observed that the sharpness of the shadow edge is not uniform. It is quite distinct at the antisolar point and becomes gradually more and more diffuse as one looks away. This effect is particularly noticeable when the mountain is an extended ridge (Fig. 6). The cause of the width variation is related to the finite angular size of the sun, the angular distance of the shadow from the antisolar point as observed from the mountain top, and the nonlinear response of the eye or film.

At the antisolar point the line of sight of the observer coincides with the sunlight. Here the line of sight vector \mathbf{r} has no x component, and the expression for the shadow profile is given by

$$I(\gamma') = 1 - \frac{1}{\pi} \cos^{-1} \left(\frac{R - \gamma'}{R} \right) - \frac{(R - \gamma')}{\pi R^2} (2R\gamma' - \gamma'^2)^{1/2}, \quad (10)$$

where γ' is the vertical coordinate. R is the angular radius of the sun. γ' has been shifted relative to γ by an amount approximately equal to α . γ' has been chosen such that at $\gamma' = 0$, $I(0) = 1$ (bright edge of the penumbra), and at $\gamma' = R$, $I(R) = 0$ (dark edge of the penumbra). The width of this profile may be defined as the full width at half maximum (FWHM) value of the first derivative of $I(\gamma')$,

$$\frac{dI}{d\gamma'} = \frac{1}{\pi} \frac{1}{[R^2 - (R - \gamma')^2]^{1/2}} + \frac{(2R\gamma' - \gamma'^2)^{1/2}}{\pi R^2} - \frac{(R - \gamma')^2}{\pi R^2 (2R\gamma' - \gamma'^2)^{1/2}}.$$

$I(\gamma')$ and $dI/d\gamma'$ are shown in Fig. 7. The FWHM is 0.43° , which is the minimum value for the width of the shadow as seen from the summit. There, at the antisolar point, the shadow appears sharpest. This is true regardless of whether the shadow is cast on the ground or on the atmospheric haze.

As one looks away from the antisolar point the line of sight no longer parallels the sunlight but rather intersects it and the plane dividing the shadow from

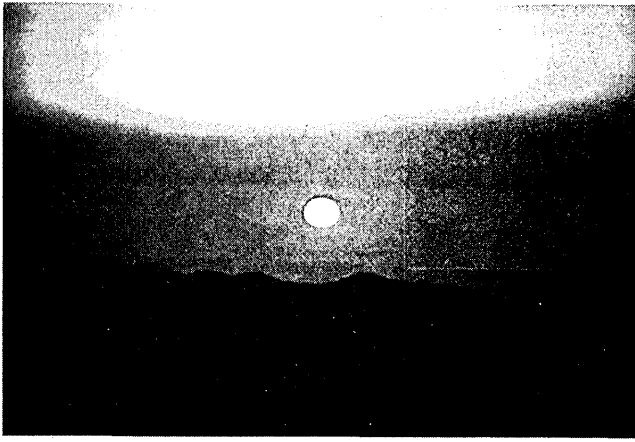


Fig. 6. The sunrise shadow of White Mountain, California, as viewed from the high altitude research laboratory. This is the special case of a flat-topped summit, which is effectively infinite in extent.



Fig. 8. Sunset shadow of Mauna Loa as seen from the weather station, approximately 16 km from the summit.

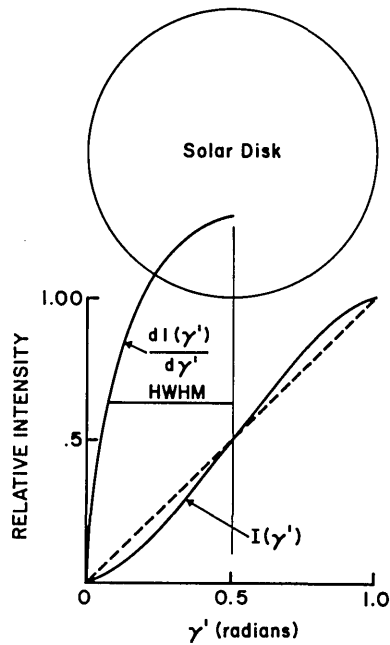


Fig. 7. Diagram used for deriving the effective width of the sun as a light source.

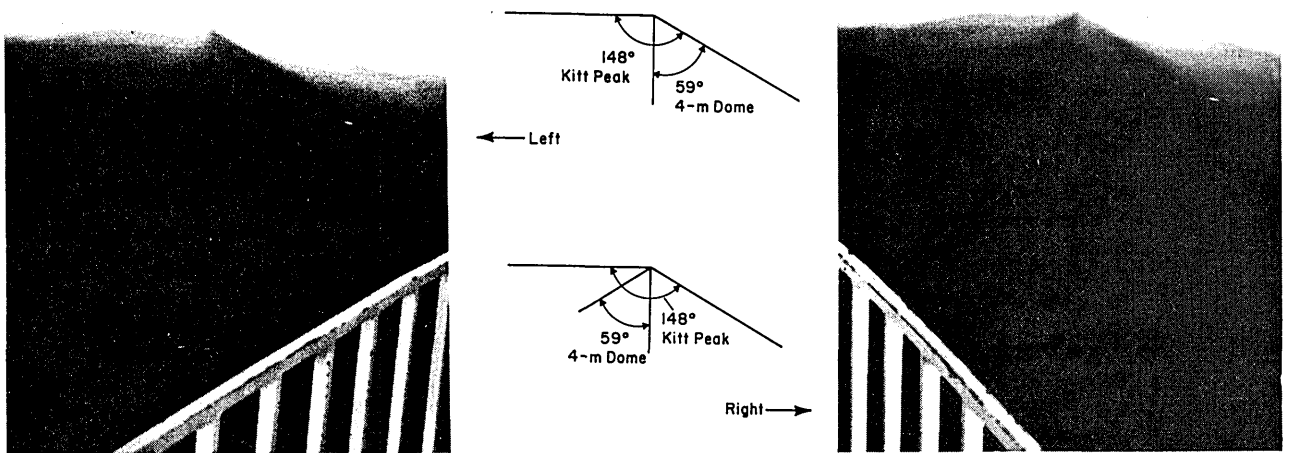


Fig. 9. Two views of the shadow of Kitt Peak as modified by the presence of the 4-m telescope dome (photograph by G. Ladd).

sunlight at an oblique angle. This introduces a significant $x[\chi]$ component into the expression for $I(\gamma')$. Furthermore, the shape of the terrain becomes important in determining the apparent width of the shadow, and the shadow edge becomes much wider than 0.43° .

In practice the shadow often appears sharper than the above theory would predict. It is as though the shadow had no penumbra, and only the umbra played a role. For example, note the narrowness of the antisolar point shadow compared with the 0.5° full moon as seen in Fig. 6. Perhaps this is a consequence of the nonlinear response of the eye or photographic film, but this should be studied further.

Shadow on the Haze

Mountain shadows commonly appear to be cast upon the haze in the atmosphere rather than on the ground. This is seen especially when the sun is very low, and the optical path through the haze is of order unity or larger. The shadow appears to rise as part of the earth shadow, acquiring the characteristic deep blue hue in contrast to the delicate pink just above it. Since the previous analysis was performed for shadows on the ground, one might ask if it is also applicable to shadows on haze. The answer is yes, providing again that one does not look too far from the antisolar point. By looking off axis the line of sight passes through the plane of the shadow edge, and since there is an $x[\chi]$ component, the width may appear larger.

Related Observations

Many mountains are not symmetric so that the top is closer to one foot than the other. Calculation indicates the shadow will be proportionally affected (Fig. 5), and observations bears this out [Fig. 1(b)]. If the observer is distant from the summit but still within the mountain mass, the pyramidal shadow persists, and apex angle A is unaffected (Fig. 8). The vertex of the shadow is, however, diffuse. This agrees with the notion that only the antisolar point is sharp.

Under certain conditions of haze, major summit features become discernible. For instance, the housing of the 4-m telescope on Kitt Peak can introduce a structured pattern to the mountain shadow (Fig. 9). At times of very clear air such effects are not seen. We conclude that haze can reduce the distance to the antisolar point allowing a partial resolution of summit detail.

Summary of Rules for Low Sun Mountain Shadows

- (1) All mountain peaks produce pyramidal shadows.
- (2) Apex angle of the shadow is $A \approx 2 \tan^{-1} (\bar{W}/Z_t)$, which is independent of the observer's position.
- (3) The shadow is sharpest around the antisolar point.
- (4) Under hazy conditions major summit features produce secondary shadows that follow (1) and (2).
- (5) If the observer is on a slope of the mountain, (1) and (2) apply, but the shadow of the side distant from the observer is fuzzy.

We acknowledge the stimulus provided by Kathy DeGioia, University of Wyoming, who inquired of us why the shadows are pyramidal. Pierre Turon, Gary Ladd, Frank Recely, and Martin Cohen contributed photographs, and E. Hiei, Tokyo Astronomical Observatory, found the material on Mt. Fuji.

Kitt Peak National Observatory is operated by the Association of Universities for Research in Astronomy, Inc., under contract with the National Science Foundation.

References

1. M. Minnaert, *I. Licht en Kleur in het landschap* (Thieme and Cie, Zutphen, 1968).
2. (Anon.), Mt. Washington Obs. Bull. 14, 52 (1973).
3. (Anon.), Mt. Fuji, Japan Times, Ltd. Tokyo (1970).
4. H. Arakawa, *Weather* 16, 220 (1961).